Drug Design, Development and Therapy

Dovepress

open access to scientific and medical research

Open Access Full Text Article

ORIGINAL RESEARCH

Polygonum Cuspidatum Alcohol Extract Exerts Analgesic Effects via the MAPK/ERK Signaling Pathway

Yan Lan[1,2,*], Yu-Kun Zheng[3,*], Liu-Yi Wu[3], Zi-Jun Zhou[3], Ruo-Xin Guan[3], Heng Xu[3], Ji-Yuan Tu[3], Xin Gu[3], Rui Wang[3], Nan Jiang[3], Yuan Wu[4], Cheng-Ren Shu[1,2], Zhong-Shi Zhou[3]

[1]Department of Pharmacy, Huangshi Central Hospital, Affiliated Hospital of Hubei Polytechnic University, Huangshi, Hubei, People's Republic of China; [2]Hubei Key Laboratory of Kidney Disease Pathogenesis and Intervention, Hubei, People's Republic of China; [3]College of Pharmacy, Hubei University of Chinese Medicine, Wuhan, Hubei, People's Republic of China; [4]Department of Radiation Oncology, Hubei Cancer Hospital, Tongji Medical College, Huazhong University of Science and Technology, Wuhan, Hubei, People's Republic of China

*These authors contributed equally to this work

Correspondence: Cheng-Ren Shu, Department of Pharmacy, Huangshi Central Hospital, NO. 141, Tianjin Road, Huangshi, Hubei, People's Republic of China, Tel +86-27-13986590438, Email 397112615@qq.com; Zhong-Shi Zhou, College of Pharmacy, Hubei University of Chinese Medicine, No. 1, Huangjiahu West Road, Hongshan District, Wuhan City, Hubei Province, People's Republic of China, Tel +86-27-15871745189, Email monkeyzzs@126.com

Objective: Traditional Chinese medicine *Polygonum cuspidatum* (PC) has significant effects on reducing pain. In this study, we investigated the analgesic effects of the alcohol extract of PC on three types of inflammatory pain and explored its mechanism.

Methods: Potential targets for the analgesic effects of the main active components of PC alcohol extract were screened by network pharmacology and molecular docking. Three different inflammatory pain mouse models (acetic acid twisting, formalin foot swelling, and xylene ear swelling) were used to study the analgesic effects of PC. The expression of latent signaling pathways in L_{4-6} spinal cord tissues in formalin foot swelling mice was evaluated using real-time qPCR (RT-qPCR), Western blot (WB), and immunohistochemistry (IHC) analyses.

Results: Network pharmacology analysis shows that PC analgesic mechanism is related to the MAPK/ERK signaling pathway. The five main active components of PC have good docking ability with JNK and p38. PC alcohol extract significantly reduced the pain behavior and alleviated inflammatory reactions in three mouse models, inhibited the mRNA and protein phosphorylation levels of JNK, ERK, p38, and CREB in spinal cord tissues.

Conclusion: PC alcohol extract can inhibit inflammation and alleviate pain, which is related to its inhibition of the MAPK/ERK signaling pathway in spinal cord. Thus, PC alcohol extract is a promising candidate for pain treatment.

Keywords: *Polygonum cuspidatum*, network pharmacology, MAPK/ERK, analgesic

Introduction

Pain is one of the most common clinical symptoms, and the interaction between both acute and chronic pain and negative emotions makes pain a leading global health problem.[1] Inflammatory pain, which represents the perception of harmful stimuli that occur during inflammation or an immune response, is the most important type of pain.[2–4] Due to cellular damage and metabolic abnormalities during inflammation, an acidic environment is formed locally in the area of inflammation, which activates peripheral nociceptors and, in turn, NLRP3 inflammasomes.[5] Inflammatory factors produced in response to NLRP3 activation, include TNF-α, 1L-6, and IL-1β. These inflammatory cytokines then activate their corresponding receptors on sensory neurons, further triggering downstream signaling pathways such as protein kinase C (PKC) and mitogen-activated protein kinases (MAPK) in cells to cause hyperalgesia leading to inflammatory pain.[6,7] Moreover, inhibiting the expression of inflammatory factors can reduce pain.[8] Pain can be a huge personal and financial burden, and understanding the mechanism of pain production is critical for identifying and developing analgesic drugs.[9,10]

Received: 4 May 2023
Accepted: 4 October 2023
Published: 19 October 2023

Polygonum cuspidatum (PC) is a common Traditional Chinese medicine (TCM) that has been used in China for thousands of years.[11] The main active components of PC include polydatin and resveratrol, which have been confirmed to have a wide range of pharmacological effects, such as anti-peroxidation and regulation of lipid metabolis.[12–14] Research has shown that PC has good analgesic activity, but the specific mechanism is not yet clear.

The dorsal horn of the spinal cord is the first station for the transmission and regulation of pain messages and contains specific pain neurons. Ectopic firing of neurons is a major cause of inflammatory pain. Expression of extracellular regulated protein kinases (ERKs) and their key upstream and downstream genes, as well as the activation and expression of proteins, plays an important role in pain transmission.[15] The mitogen-activated protein kinase (MAPK)/ERK signaling pathway in the dorsal horn of the spinal cord is an important marker of pain transmission[16,17] and is implicated as a potential target by which the analgesic effects of PC are mediated.

The main active components and compound preparations of PC have significant efficacy in the treatment of pain-related diseases such as gouty arthritis,[18,19] but the specific mechanism of action is not clear. In this study, we used high performance liquid chromatography (HPLC) to analyze the main active components of PC alcohol extract and screen its possible targets using a network pharmacology approach. We also used different inflammatory pain models to verify the efficacy and potential targets of PC alcohol extract, to provide a theoretical basis for improved implementation of the analgesic effects of PC.

Materials and Methods

Preparation of Alcohol Extract of PC

PC Yinpian samples were obtained from Fangxian County, Hubei Province, China (product batch number 191104), which were processed in accordance with the Chinese Pharmacopoeia, 2020 edition. The authenticity of PC Yinpian samples were identified by Yimei Liu (Professor of Hubei University of Chinese Medicine). The voucher specimen (No. 4203251205150015LY) is stored in the Herbarium of Hubei University of Chinese Medicine. The alcohol extract of PC was prepared according to a previously study method.[20] Briefly, 10 volumes of 70% alcohol were added to an appropriate amount of decoction pieces of PC and the extraction was performed twice by refluxing, first for 1 h and then by 0.5 h. The filtrates were combined and the extract was dried using a rotary-evaporated under reduced pressure to obtain the dry powdered alcohol extract of PC, which was then dissolved in water for use as a reagent in our studies.

HPLC Analysis

A mixed control solution was prepared by dissolving the following in methanol: polydatin (Chengdu Herbpurify, cat#H-012-171216, China), resveratrol (Chengdu Herbpurify, cat# B-002-170426), emodin-8-O-β-D-glucoside (Chengdu Herbpurify, cat# D-018-171216), emodin (Shanghai yuanye Bio-Technology, cat# T17A10F95418, China), and physcion (Shanghai yuanye Bio-Technology, cat# T26A8F34784).

An appropriate amount of PC alcohol extract powder was passed through the No. 3 sieve into an Erlenmeyer flask and dissolved in 60% alcohol. The solution was then subjected to ultrasound (power 250 W, frequency 40 kHz) for 30 min, cooled to room temperature and weighed. Subsequently, 60% alcohol was added to compensate for the weight lost during processing before the solution was mixed by shaking and using 0.22 μm microporous membrane filtered. A 10-μL aliquot of the continuous filtrate was then used as the test solution.

The HPLC (Agilent 1260 liquid chromatograph, China) analysis conditions were then optimized according to a previously described method[21] Briefly, the following conditions were used: column was filled with octadecyl silane-bonded silica gel (Agilent Extend C18 chromatographic column, 250 mm × 4.6 mm, 5 μm, China); mobile phase A, acetonitrile; mobile phase B, water; detection wavelength, 290 nm; column temperature, 40°C; injection volume, 10 μL; gradient elution process, 0–22 min at 15.0–35.0% A followed by 22–40 min at 35.0–100.0% A.

Network Pharmacology Analysis

Screening of Targets of the Main Active Components of PC

The chemical abstracts service (CAS) numbers of the five main active components of PC obtained by HPLC were input into PubChem (https://pubchem.ncbi.nlm.nih.gov). Data for the "Canonical SMILES" structural formula of the chemical compound in PubChem were then input into SwissTargetPrediction (http://www.swisstargetprediction.ch) with the species limited to "Homo sapiens" and all targets were downloaded. The main active component table of PC was used to match the corresponding target gene name and duplicate values were eliminated to obtain a complete list of potential targets of the main active components of PC.

Disease Target Search and Common Target Screening

The use of the database was approved by the Medical Ethics Committee of Huangshi Central Hospital. The GeneCards human gene database (https://www.genecards.org) and OMIM human genes and genetic disorders database (https://www.omim.org) were searched using the keyword "Analgesia" and Venny 2.1.0 (https://bioinfogp.cnb.csic.es/tools/venny/index.html) was used to visualize the output as a Venn diagram of the screened disease and drug targets and identify the common disease and drug targets.

Construction of PC Main Active Component-Analgesic Target Network

The common targets were then input into the STRING database (https://cn.string-db.org) for PPI network construction, with the biological species set to "Homo sapiens", and the confidence level set to "≥0.9". To more intuitively visualize the relationship of PC components and pain with corresponding targets, the Drug-Component-Target network diagram was constructed using Cytoscape 3.9.1 software.

Molecular Docking Simulation

The 3D structure PDB format files for the MAPK8 and MAPK14 (PDBID:3PZE/1OUY) proteins were downloaded from the RSCB PDB database (https://ww.rcsb.org/)[22] The SDF format files of small molecules were downloaded from PubChem database, and the format was converted using Open Babel software. Taking proteins as receptors and small molecules as ligands, the AutoDockTools 1.5.6 in Discovery Studio was used to determine the active pockets of receptors and molecular docking simulation was performed using AutoDock Vina.[23] The docking results were visualized with PyMol software.

Animal Model Grouping and Dosing

ICR mice (female, specific pathogen-free, aged 6–8 weeks, weight 18–22 g; n = 150) were divided into the following groups (n = 30 per group): control (Ctrl), model (Mod), low-dose PC (HD), high-dose PC (HG), and positive control aspirin (AS). The HD and HG groups received intragastric administration of 2 $g \cdot kg^{-1}$ and 8 $g \cdot kg^{-1}$ of PC raw drug content, while the AS group received 0.1 $mL \cdot 10\ g^{-1}$ aspirin solution and the Ctrl and Mod groups received a gastric perfusion of an equal volume of normal saline.

Analgesic Model Studies

Acetic Acid Writhing Model

The model was established as previously described.[24] At 30 min after the end of intragastric administration (n = 10 mice per group), the Ctrl group received an intraperitoneal injection of 0.9% normal saline solution, while the other groups were intraperitoneally injected with 1% acetic acid solution (all 0.2 $mL \cdot 10\ g^{-1}$). The time of the first occurrence of writhing was recorded (writhing latency time) as well as the times of writhing reactions in mice within 30 min after intraperitoneal injection. The rate of writhing inhibition as calculated as (writhing times of Mod group - writhing times of drug administration group)/average writhing times of Mod group × 100%.

Formalin Foot Swelling Model

The model was established as previously described.[25] At 30 min after the end of intragastric administration (n = 10 mice per group), the Ctrl group received 20 μL 0.9% normal saline solution injected into the right posterior plantar surface, while the

remaining groups received the same volume of 1.0% formalin solution injected into the same site. The biphasic pain reaction of the paws after licking was observed and recorded for a period of 60 min, with 0–10 min defined as Phase I, and 10–60 min defined as phase II. After the observation period, mice were sacrificed by cervical dislocation and the $L_{4\text{-}6}$ spinal cord collected.

Xylene Ear Swelling Study

The model was established as previously described.[26] At 30 min after the end of intragastric administration (n = 10 mice per group), the Ctrl group received 20 μL 0.9% normal saline solution applied evenly on both sides of the left ear, while the remaining groups of mice received the same volume of xylene solution applied to the same region. After 1 h, all mice were euthanized by cervical dislocation, and the ears removed, and weighed separately. The ear weight difference was calculated as the weight of left ear – the weight of right ear.

RT-qPCR Analysis

Total RNA was extracted from spinal cord tissues using TRIzol reagent (Thermo Fisher Scientific, cat#10296010) according to the manufacturer's instructions. Relevant primers were designed using NCBI (https://www.ncbi.nlm.nih.gov), and the sequences are shown in Table 1. Total RNA was reverse transcribed to cDNA using a reverse transcription kit (Vazyme, cat#R223-01) and the amplification system was configured using an amplification kit (Abclonal, cat#RK20429). Gene expression was analyzed using a PCR system (Analytik Jena, Germany) using a three-step protocol as follows: predenaturation at 95°C for 1 min followed by 40 cycles of denaturation at 95°C for 20s and annealing/extension at 60°C for 45s and reaction at 95°C for 1 min. Data were normalized against β-actin before the relative gene expression was determined using the $2^{-\Delta\Delta Ct}$ method.

Table 1 Primer Sequence Listing

ID	Primer	Primer Sequence(5'to3')	Base Number
1	β-actin-F-Mus	TGTACCCAGGCATTGCTGAC	20
2	β-actin-R-Mus	AACGCAGCTCAGTAACAGTCC	21
3	TNF-α-F-Mus	ATGGCCTCCCTCTCATCAGT	20
4	TNF-α-R-Mus	TTTGCTACGACGTGGGCTAC	20
5	NLRP3-F-Mus	CTCGTCACCATGGGTTCTGGT	21
6	NLRP3-R-Mus	AACGGACACTCGTCATCTTCA	21
7	IL-6-F-Mus	GCTGACTTGAGGAGGCAGTT	20
8	IL-6-R-Mus	TCAATCTCCAGCGACAGCAG	20
9	IL-1β-F-Mus	TGCGTCATCCATGATGCCTT	20
10	IL-1β-R-Mus	CCTGGGCTCTGCTATCCAAG	20
11	JNK-F-Mus	AACGCAGCTCAGTAACAGTCC	21
12	JNK-R-Mus	TGTGCTAAAGGAGACGGCTG	20
13	ERK-F-Mus	TAAATTGGTCAGGACAAGGGCT	22
14	ERK-R-Mus	AGAGTGGGTAAGCTGAGACG	20
15	p38-F-Mus	AGAGTGGGTAAGCTGAGACG	20
16	p38-R-Mus	TTCTTCAGAAGCTCAGCCCC	20
17	CREB-F-Mus	GAGAAGCGGAGTGTTGGTGA	20
18	CREB-R-Mus	ACTCTGCTGGTTGTCTGCTC	20

Western Blot Analysis

Western blot analysis was performed following standard protocols. Proteins from the extracted spinal cord tissues were separated by sodium dodecyl sulfate-polyacrylamide gel electrophoresis (SDS-PAGE, 10% gel), and then transferred to polyvinylidene fluoride (PVDF) membranes (pore size 0.45 μm). After blocking in 5% dried skimmed milk solution for 1 h, the membranes were incubated at 4°C for 8 h with the following primary antibodies diluted in 5% dried skimmed milk/TBS Tween 20 (1%) buffer (TBS-T): anti-β-actin (Cell Signaling, cat#12620, 1/10000) as a loading control, anti-p38 (Cell Signaling Technology, cat#9212, 1/1000), anti-p-p38 (Cell Signaling Technology, cat#9211, 1/1000), anti-ERK (Cell Signaling Technology, cat#4695, 1/1000), anti-p-ERK (Cell Signaling Technology, cat#9101, 1/1000), anti-JNK (Cell Signaling Technology, cat#9252, 1/1000), anti-p-JNK (Cell Signaling Technology, cat#4668, 1/1000), anti-CREB (Zenbio, cat#381013, 1/1000), and anti-p-CREB (Zenbio, cat#340731, 1/1000). Membranes were then washed with TBS-T buffer, followed by incubation with goat anti-rabbit IgG antibody (Solarbio, cat#SE134, 1/5000) for 1 h at room temperature. Protein bands were developed with ECL chemiluminescence solution (Solarbio, cat#A6856), visualized using a gel imaging system (ProteinSimple, USA) and quantified by measurement of the grayscale values of each band using ImageJ software.

IHC Staining

Paraffin-embedded spinal cord tissues sections were dewaxed, hydrated and incubated with the p-JNK/p-p38 antibodies used for Western blot analysis. After incubation with the DAB Chromogenic Kit (Dako, cat#K5007) according to the manufacturer's instructions, the sections were counterstained with hematoxylin (Solarbio, cat#H8070-5g) for 3 min, rinsed with distilled water, and returned to blue using a blue-returning solution. The average optical density (AOD) of the positively-stained area was detected using the ImageJ software.

ELISA Detection

Based on the manufacturer's instructions, use an ELISA detection kit to detect the relative expression of 1L-6 (Elabscience, cat#E-EL-M0044c) and 1L-1β (Neobioscience Technology Co, Ltd, cat#EMC001b. 96) in mouse serum.

Statistical Analysis

Statistical analysis was performed using GraphPad Prism 8.0 software (GraphPad Soft, USA). Two groups were compared using the Student's *t*-test and multiple groups were compared using one-way ANOVA. Unless otherwise stated, all in vitro experiments are repeated three times and results were expressed as mean ± standard deviation (SD). $P \leq 0.05$ was considered to indicated statistical significance.

Results

Analysis of PC Alcohol Extract Components

To investigate the material basis of the analgesic effects of PC alcohol extract, the composition of PC alcohol extract was analyzed by HPLC (Figure 1A). Combined with the mixed standard atlas (Figure 1B), five main active components were identified at relatively high levels in the PC alcohol extract: polydatin (1), resveratrol (2), emodin-8-o-β-D-glucoside (3), emodin (4) and physcion (5).

Network Pharmacology Analysis of the Main Active Components of PC

Searches of the SwissTargetPrediction database revealed 350 PC-related targets for the five main active components of PC, and 370 analgesia-related targets were identified in the GeneCards and OMIM database; 58 common targets were identified (Figure 2A). Arrangement of the targets according to the value related to PC relevance and further correlation with the components of PC revealed significant enrichment of TNF, MAPK8 (JNK) and MAPK14 (p38) (Figure 2B and C). KEGG analysis revealed enrichment in neuroactive ligand-receptor interaction and the TNF signaling pathway (Figure 2D), and GO analysis revealed enrichment of the MAPK signaling pathway in the biological process (BP) category (Figure 2E).

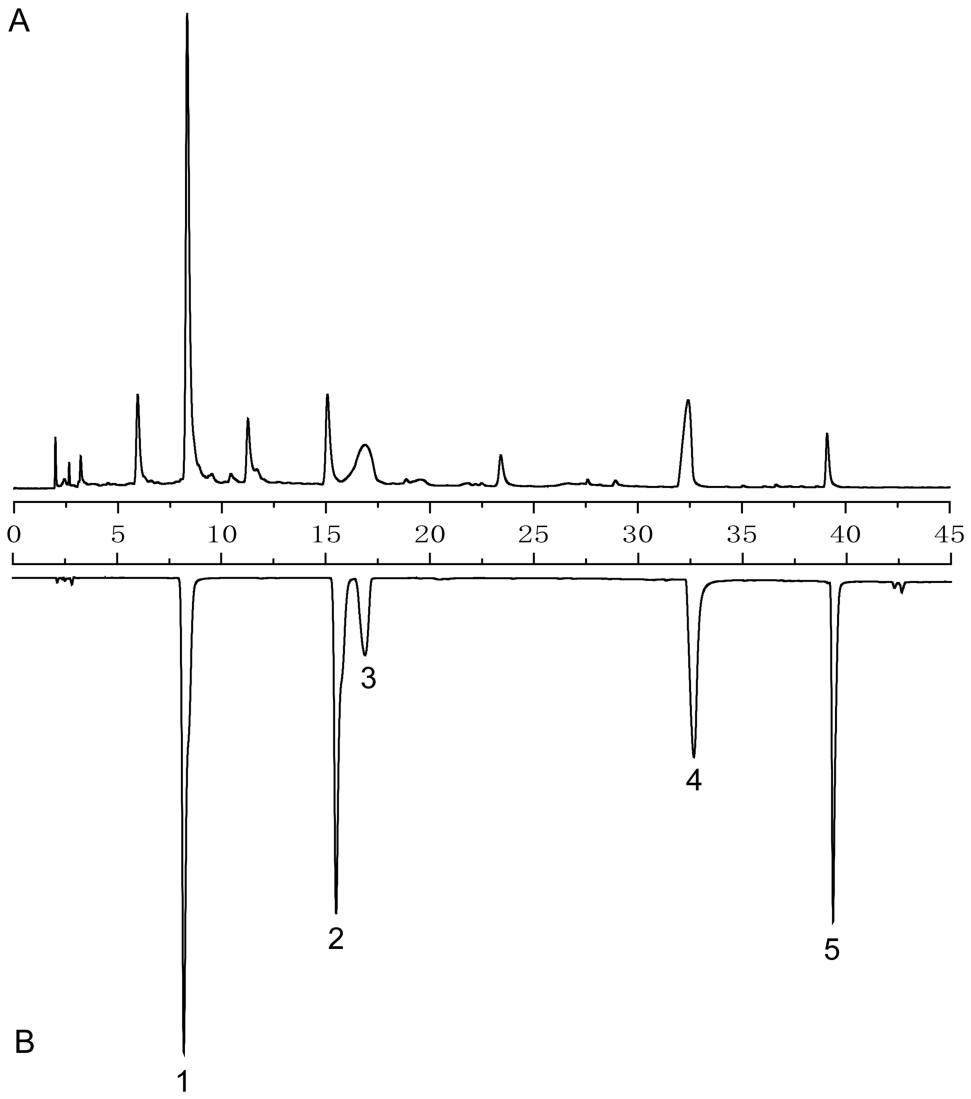

Figure 1 Image contrast diagram of PC alcohol extract and mixed standard. (**A**) HPLC chromatogram of alcohol extract of PC. (**B**) HPLC chromatogram of mixed standard. 1 polydatin, 2 resveratrol, 3 emodin-8-o-β-D-glucoside, 4 emodin, 5 physcion.

Molecular Docking Simulation of the Main Active Components with JNK/p38 Molecules

The interactions of the five main active components of PC and the MAPK signaling pathway were then further evaluated using molecular docking simulation technology and the vina scores were calculated. All five components of PC showed good docking activity with JNK and p38 (vina scores ≤-7) (Figure 3A–J). According to the vina scores, the range of binding abilities of the five main active components of PC to JNK from strong to weak was: physcion, emodin, emodin 8-O-β-D-glucoside, polydatin, resveratrol (Table 2). The range of binding abilities of the main active components of PC to p38 is from strong to weak was: emodin, physcion, polydatin, resveratrol, emodin 8-O-β-D-glucoside (Table 3).

Analgesic Effects of PC Alcohol Extract

The analgesic effects of PC alcohol extract were evaluated using the acetic acid twisting, formalin foot swelling and xylene ear swelling models, with AS as the positive control. In the acetic acid twisting model, the twisting reaction occurred for the first time approximately 3 min after intraperitoneal injection of acetic acid solution in the Mod group. In the HD, HG and AS groups, the twisting latency time was extended (Figure 4A) and the number of twisting reactions was reduced ($n \geq 5$, $P < 0.01$)

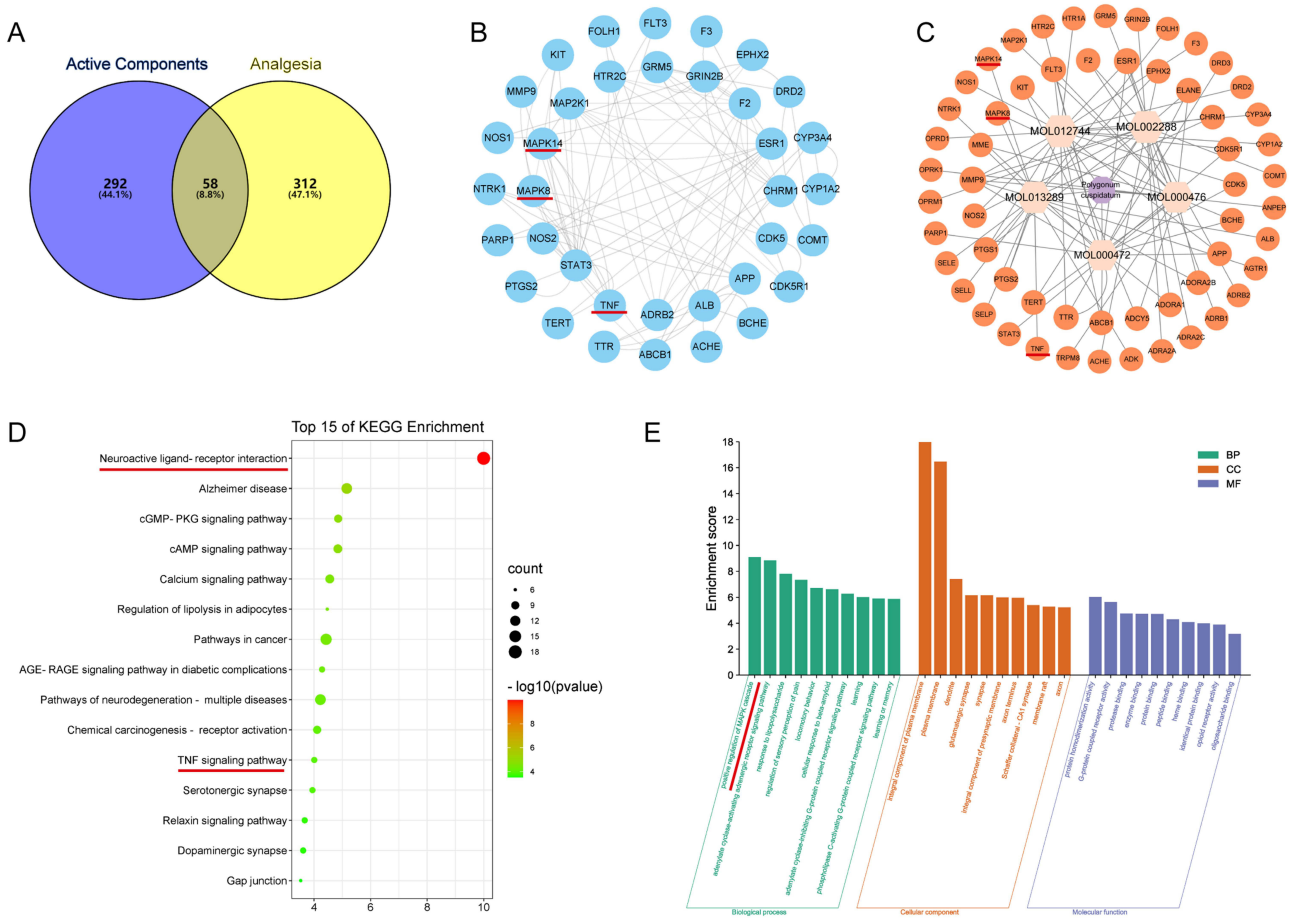

Figure 2 Five main active components of PC - analgesic network pharmacological study. (**A**) Venn diagram showing the analgesia common targets of the five main active components of PC. (**B**) Analysis of the PPI network of the five main active components of PC and analgesia common targets. (**C**) PC-component-target network diagram. (**D**) KEGG enrichment analysis of the five main active components of PC and analgesia common targets. (**E**) GO enrichment analysis of the five main active components of PC and analgesia common targets.

(Figure 4B). The twisting reaction of mice was also significantly inhibited in the HD, HG and AS groups ($n \geq 5$, $p < 0.01$) (Figure 4C). In the formalin foot swelling model, two distinct phases of reactions occurred after formalin injection into the plantar region of the mouse. Immediately after the injection ended, the mice began to lick the soles of the feet intermittently, this reaction gradually disappeared after 10 min. After 20 min, the mice began to lick the soles of their feet intermittently again, and this reaction disappeared after 60 min. Our experimental data showed that the Phase I licking time was significantly reduced in the HG and AS groups ($n \geq 5$, $P < 0.01$) but not in the HD group (Figure 4D). The phase II licking time was significantly reduced in the HD, HG and AS groups ($n \geq 5$, $p < 0.01$) (Figure 4E). In the xylene ear swelling model, the ear swelling was reduced to varying degrees in the HD, HG and AS groups ($n \geq 5$, $P < 0.01$) (Figure 4F). The HD, HG and AS groups also significantly improved the plantar inflammatory swelling caused by formalin plantar injection ($n \geq 5$) (Figure 4G).

Effects of PC Alcohol Extract on Expression of Genes Related to Inflammation and the MAPK/ERK Signaling Pathway

ELISA detection found that the HD, HG and AS groups significantly reduced the expression of 1L-6 and 1L-β in mouse serum ($n \geq 3$, $P < 0.01$) (Figure 5A and B). Furthermore, RT-qPCR analysis of the L_{4-6} spinal cord tissues of mice in the formalin foot swelling model showed that the expression of the inflammation-related genes TNF-α, NLRP3, 1L-6, and 1L-β was significantly increased in the Mod group ($n \geq 3$, $P < 0.01$), while the expression of these inflammatory factors was significantly reduced in the HD, HG and AS groups ($n \geq 3$, $P < 0.01$) (Figure 5C–F). Expression of the JNK, ERK, p38 and CREB genes related to the MAPK/ERK signaling pathway was significantly increased in the Mod group ($n \geq 3$, $P < 0.05$) and significantly reduced in both

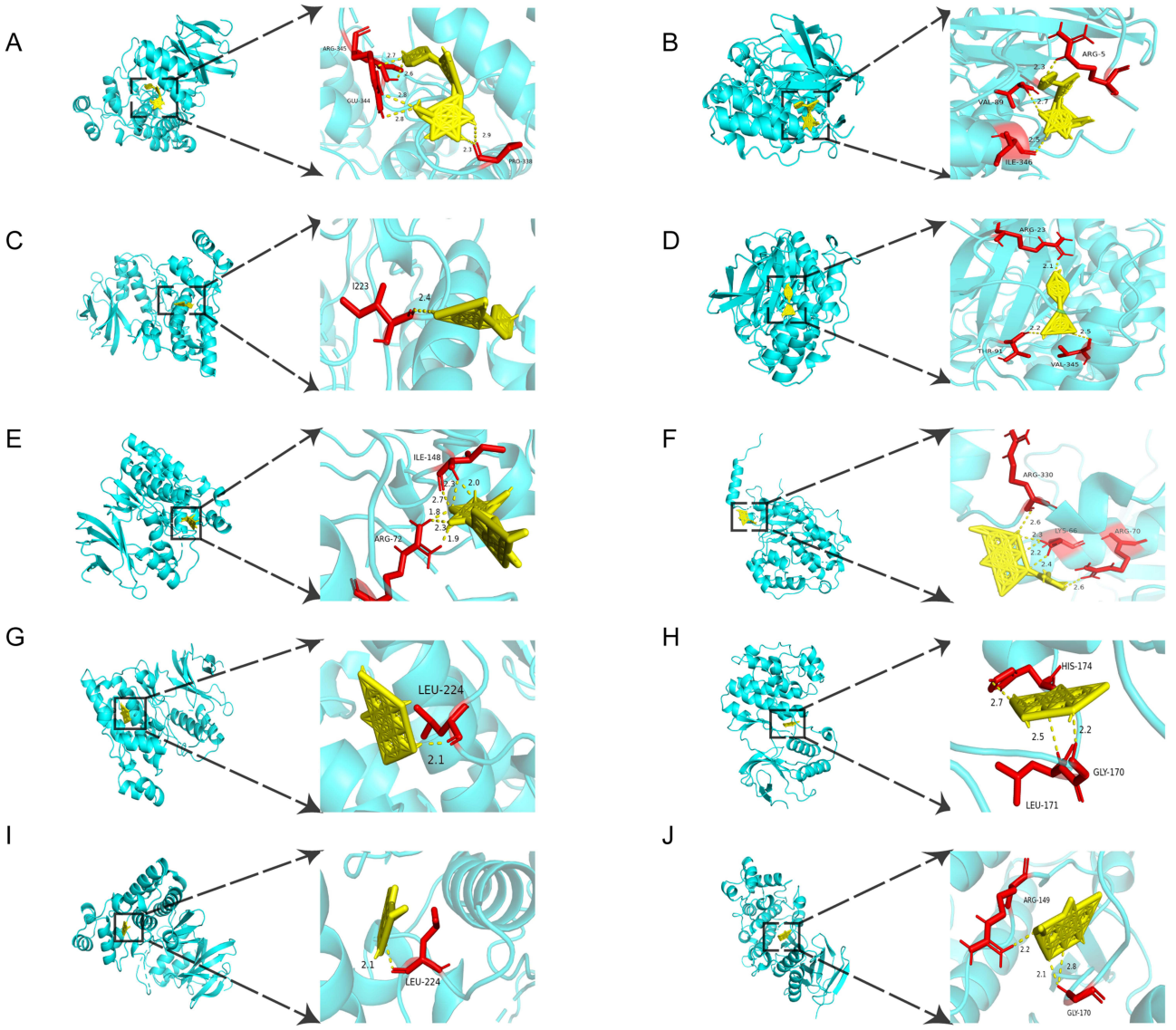

Figure 3 3D schematic diagram of the molecular docking simulation of the five main active components of PC with JNK/p38 (Human sources) molecules. Molecular docking mode diagram of polydatin with JNK (**A**) and p38 (**B**). Molecular docking mode diagram of resveratrol with JNK (**C**) and p38 (**D**). Molecular docking mode diagram of emodin-8-o-β-D-glucoside with JNK (**E**) and p38 (**F**). Molecular docking mode diagram of emodin with JNK (**G**) and p38 (**H**). Molecular docking mode diagram of physcion with JNK (**I**) and p38 (**J**).The dashed line represents the region where small molecules bind to proteins. Letters represent the names of amino acid residues. Numbers represent the length of hydrogen bonds.

the HD and HG groups ($n \geq 3$, $P < 0.05$), while there was no significant change in the expression of p38 and CREB in the AS group (Figure 5G–J).

Effects of PC Alcohol Extract on Expression of Proteins Associated with the MAPK/ERK Signaling Pathway

To investigate the effects of PC alcohol extract on the protein expression of genes related to the MAPK/ERK signaling pathway, we performed WB analysis on the levels of JNK, ERK, p38, and CREB and their phosphorylated proteins in the spinal cord tissue of formalin foot swelling model mice (Figure 6A). The phosphorylated levels of the four proteins were downregulated in the HD and HG groups compared with those in the Mod group ($n \geq 3$, $P < 0.05$), while there were no significant changes in the levels of the four phosphorylated proteins in the AS group (Figure 6B–E). The results of the network pharmacology analysis were confirmed by IHC staining of mouse spinal cord tissues (Figure 6F and G). The trends in the expression levels of p-p38 and p-JNK were consistent with the WB results ($n \geq 3$, $P < 0.05$) (Figure 6H and I).

Table 2 Vina Scores of the Five Main Active Components of PC Docking with JNK Molecules

Number	Ligand	CAS	Mol ID	OB%	Caco-2	DL	Receptor	Vina score	Center			Size		
									X	Y	Z	X	Y	Z
1	Physcion	521-61-9	MOL000476	22.29	0.52	0.27	JNK	−9.2	16	17	23	62	82	112
2	Emodin	518-82-1	MOL000472	24.4	0.22	0.24	JNK	−9.1	16	16	23	62	82	112
3	Emodin 8-O-β-D-glucoside	23313-21-5	MOL002288	44.81	−1.12	0.8	JNK	−8.2	11	11	14	68	110	114
4	Polydatin	27,208-80-6	MOL013289	21.44	−0.9	0.5	JNK	−7.7	9	11	16	98	124	126
5	Resveratrol	501-36-0	MOL012744	44.81	−1.12	0.8	JNK	−7.6	16	16	24	78	92	112

https://doi.org/10.2147/DDDT.S420002

Table 3 Vina Scores of the Five Main Active Components of PC Docking with p38 Molecules

Number	Ligand	CAS	Mol ID	OB%	Caco-2	DL	Receptor	Vina score	Center			Size		
									X	Y	Z	X	Y	Z
1	Emodin	518-82-1	MOL000472	24.4	0.22	0.24	p38	−9.0	16	16	23	126	86	118
2	Physcion	521-61-9	MOL000476	22.29	0.52	0.27	p38	−8.6	26	−5	35	64	116	98
3	Polydatin	27208-80-6	MOL013289	21.44	−0.9	0.5	p38	−8.5	19	26	−2	68	106	126
4	Resveratrol	501-36-0	MOL012744	44.81	−1.12	0.8	p38	−7.0	42	25	41	118	88	118
5	Emodin 8-O-β-D-glucoside	23313-21-5	MOL002288	44.81	−1.12	0.8	p38	−7.0	12	10	14	72	50	88

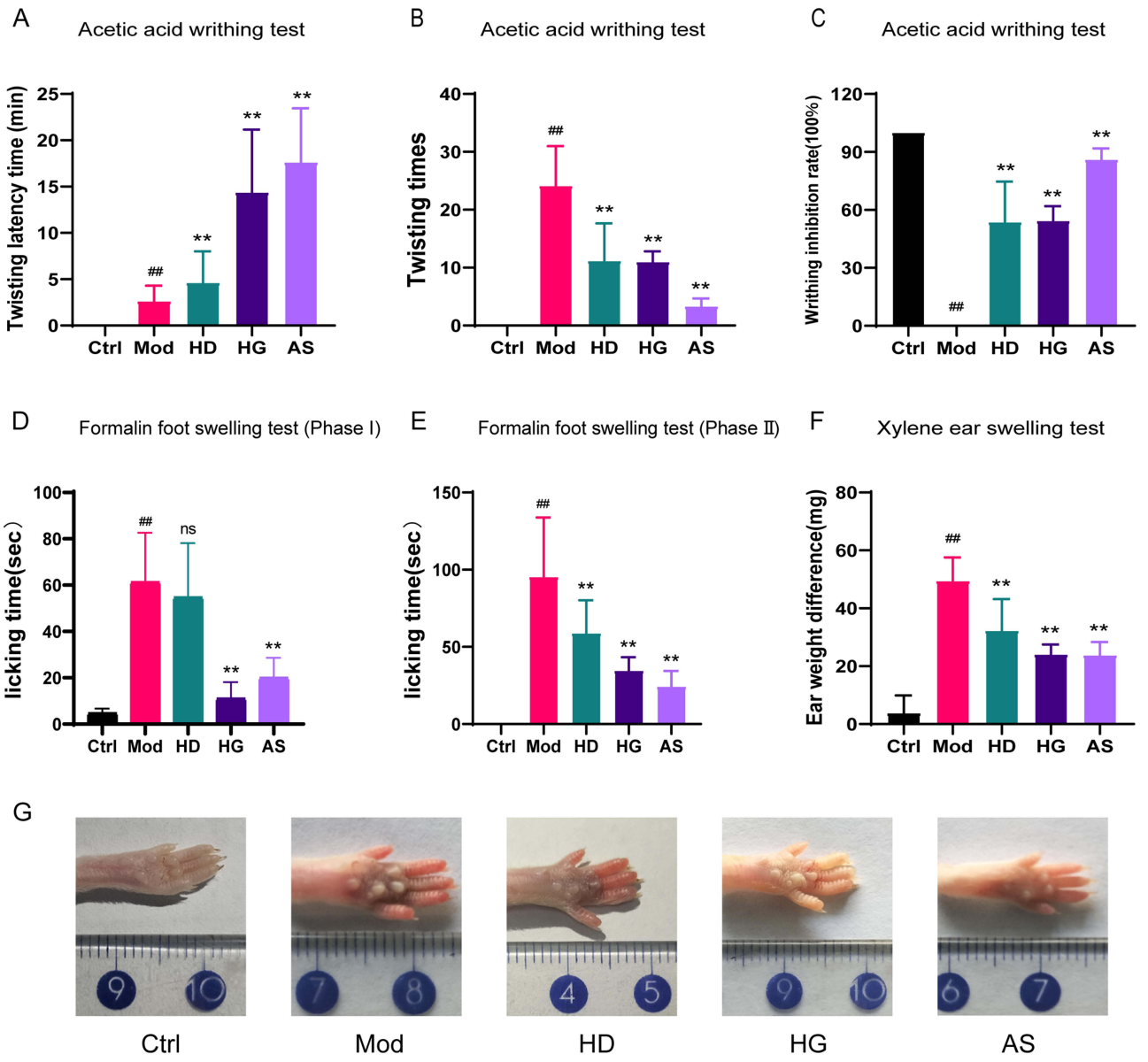

Figure 4 Analgesic pharmacodynamics study of PC alcohol extract. (**A**) Twisting latency time of mice in the control (Ctrl), model (Mod), low-dose PC (HD), high-dose PC (HG), and positive control aspirin (AS) groups in the acetic acid twisting model. (**B**) Bar graphs of the number of twists in each group in the acetic acid twisting model. (**C**) Bar graphs of the twisting inhibition rate in each group in the acetic acid twisting model. (**D**) Bar graphs of the phase I licking time in each group in the formalin foot swelling model. (**E**) Bar graphs of the phase II licking time in each group in the formalin foot swelling model. (**F**) Differences in ear weight in each group in the xylene ear swelling model. (**G**) Images of the right foot mice in the Ctrl/Mod/HD/HG/AS groups in the formalin foot swelling model. Data represent the mean ± SD (n ≥ 5). ns: not significant vs Ctrl group, $^{\#\#}P < 0.01$ vs Ctrl group, $^{**}P < 0.01$ vs Mod group.

Discussion

In this study, we identified main active components of the PC alcohol extract by HPLC and analyzed the potential analgesic targets through network pharmacology. We then verified the analgesic effects of PC alcohol extract in three different inflammatory models, and further explored the underlying mechanism through investigation of spinal cord tissues of formalin foot swelling model mice. The network pharmacology analysis suggested that the analgesic effects of PC can be related to its main active components binding to the relative protein of the MAPK/ERK signaling pathway. Furthermore, the PC alcohol extract exerted significant anti-inflammatory and analgesic effects in all three inflammatory pain models. We also showed that the expression of the MAPK/ERK signaling pathway-related genes was significantly reduced in the spinal cord tissues of formalin foot swelling model mice.

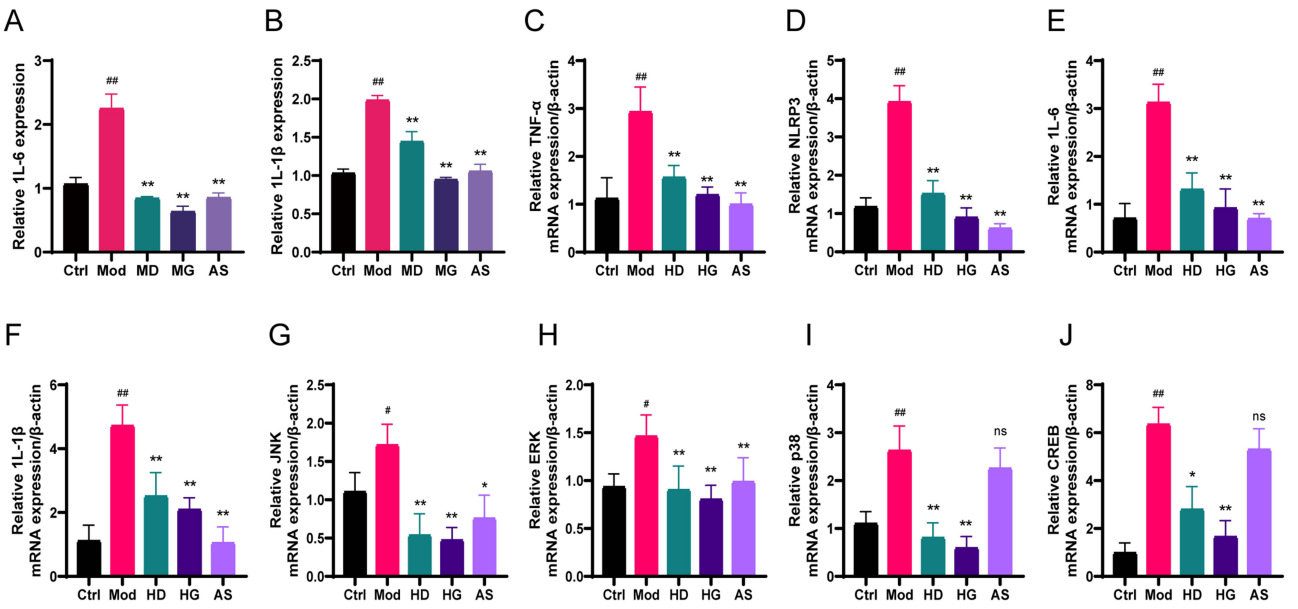

Figure 5 Effects of PC alcohol extract on expression of genes associated with the inflammation and the MAPK/ERK signaling pathway. (**A**) ELISA analysis of the gene expression of the inflammatory factors 1L-6 in serum. (**B**) ELISA analysis of the gene expression of the inflammatory factors 1L-1β in serum. RT-qPCR analysis of the gene expression of the inflammatory factors TNF-α (**C**), NLRP3 (**D**), 1L-6 (**E**), and 1L-β (**F**) in the L_{4-6} spinal cord of mice in the Ctrl/Mod/HD/HG/AS groups in the formalin foot swelling model. RT-qPCR analysis of the gene expression of JNK (**G**), ERK (**H**), p38 (**I**), and CREB (**J**) in the L_{4-6} spinal cord of mice in the Ctrl/Mod/HD/HG/AS groups in the formalin foot swelling model. Data represent the mean ± SD of three independent experiments. ns: not significant vs Ctrl group, $^{\#}P < 0.05$ and $^{\#\#}P < 0.01$ vs Ctrl group, $^{*}P < 0.05$ and $^{**}P < 0.01$ vs Mod group.

PC is used in a TCM to clear heat and dampness, reduce yellowing and disperse stasis.[27] PC active components emodin can accelerates diabetic wound healing by promoting anti-inflammatory macrophage polarization while physcion can protects rats against cerebral ischemia-reperfusion injury;[28,29] Resveratrol and polydatin can both serve as modulators of calcium mobilization in the cardiovascular system, and emodin-8-O-β-D-glucoside promotes proliferation and differentiation of osteoblastic MC3T3-E1 cells.[30,31] Modern pharmacology has also shown that the effects of PC include improving intestinal flora disorders and treating coronavirus infection.[32,33] PC has significant effects in the treatment of gouty osteoarthritis, and studies have shown that the component emodin is an important material basis for this function.[34,35] The substances and mechanisms responsible for the pain-relieving effects of PC are not yet clear. In the case of inflammatory pain, the released chemical mediators act on receptors surrounding the neurites in the Dorsal Root Ganglia (DRG), increasing the incoming discharge from the periphery to the spinal cord dorsal horn. This leads to hyperexcitability of spinal nociceptive neurons and the induction of abnormal pain and hyperalgesia.[36] Our research focuses on the crucial step of pain transmission in the spinal cord, combining HPLC, bioinformatics, and molecular biology methods to preliminarily reveal the active substances and their mechanisms of action in the pain-relieving properties of PC. Using a network pharmacology approach in this study, we provided evident that the five main active components of PC exert analgesic effects via p38 and JNK. In addition, the docking ability of emodin with p38 and JNK ranks first and second among the five components, indicating that it may be a key component in the analgesic effects of PC. The active components of PC, such as emodin and resveratrol, can enter the bloodstream through oral or injection.[37–39] Although the OB values of physcion, emodin and polydatin are all lower than the conventional 30, they are the top 5 most abundant components in PC. These substances may undergo conversion in the vivo, for example, polydatin can be converted into resveratrol for better utilization.[40] However, their transformation conditions and mechanism of action still require further. Our study provides clues to the possible distribution and metabolism of these components, and further research is expected.

Studies have shown that pain in a variety of organs such as the back, neck, and intestines is closely related to inflammation.[41,42] Unresolved inflammation can lead to chronic pain.[43] In this study, we further examined the anti-inflammatory and analgesic effects of PC in three different inflammatory pain models: a model of visceral pain (acetic acid twisting model), a model of chronic persistent inflammatory pain model (formalin foot swelling model), and an acute

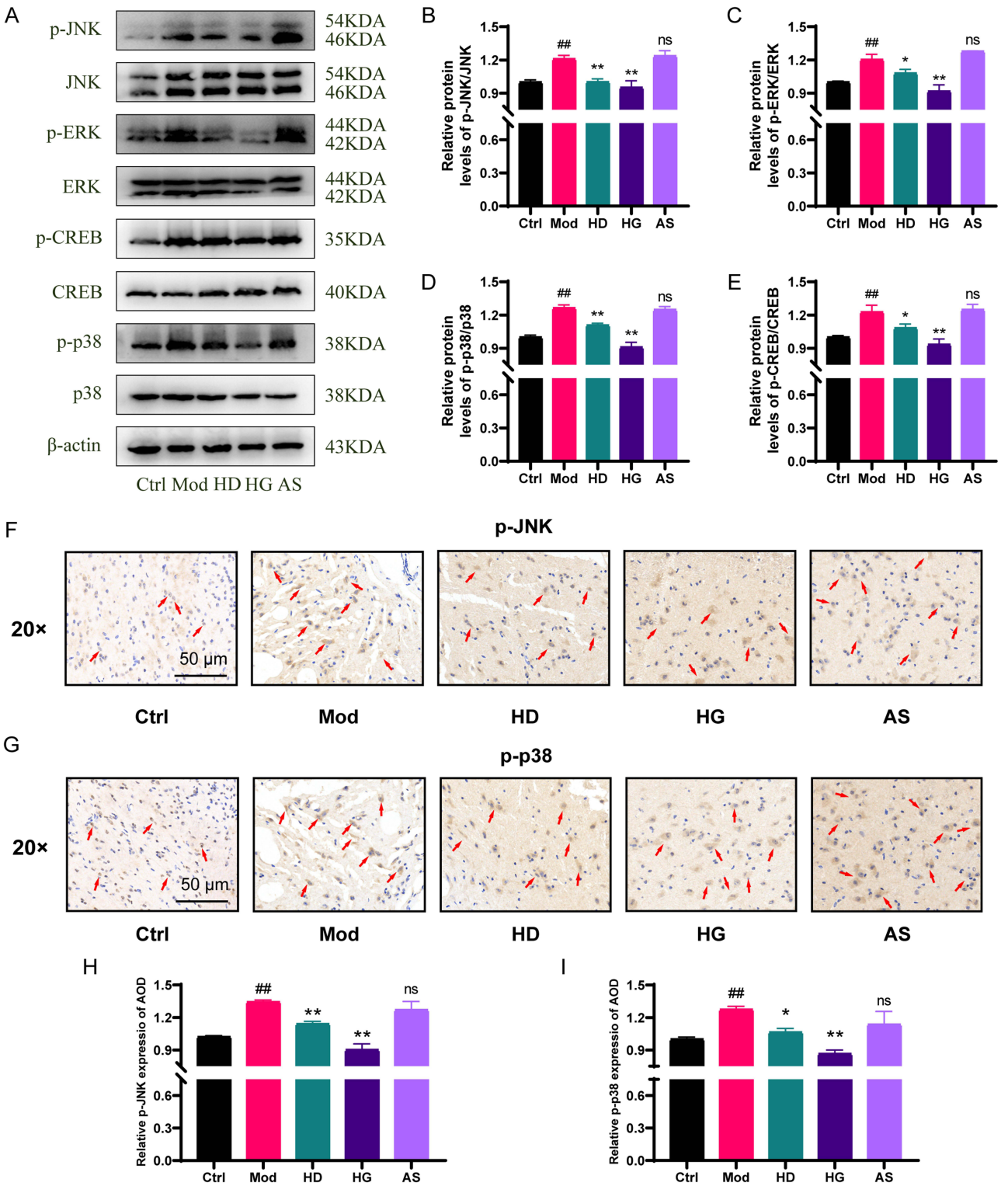

Figure 6 Effects of PC alcohol extract on proteins associated with the MAPK/ERK signaling pathway. (**A**) Western blot analysis of the expression of JNK, p-JNK, ERK, p-ERK, p38/p-P38, CREB and p-CREB protein in the $L_{4\text{-}6}$ spinal cord tissues of mice in the Ctrl/Mod/HD/HG/AS groups in the formalin foot swelling model. (**B**–**E**) Quantification of the data shown in (**A**). IHC assay for the expression of p-JNK (**F**) and p-p38 (**G**) in the mice $L_{4\text{-}6}$ spinal cord tissues mice in the Ctrl/Mod/HD/HG/AS groups in the formalin foot swelling model. (**H**) Quantification of the data shown in (**F**). (**I**) Quantification of the data shown in (**G**). Data represent the mean ± SD of three independent experiments. ns: not significant vs Ctrl group, $^{\#\#}P < 0.01$ vs Ctrl group, $^{*}P < 0.05$ and $^{**}P < 0.01$ vs Mod group.

inflammatory pain model (xylene ear swelling model). PC alcohol extract exerted analgesic effects in all three different models of inflammatory pain. In the formalin foot swelling model, HD did not significantly reduce the phase I pain response, while the licking time of Phase II was reduced in both the HD and HG groups. Studies have shown that phase I licking time is associated with neurogenic responses, and phase II licking time is associated with inflammation.[44] Our detection of inflammatory factors expression in spinal cord tissues further indicates that pain stimulation can lead to the secretion of inflammatory factors in spinal cord tissues, and PC alcohol extract can alleviate inflammation and inhibit pain.

The MAPK/ERK signaling pathway plays important roles in initiating and regulating a variety of processes, including neural plasticity, learning and memory. Moreover, along with multiple intracellular signaling pathways, the MAPK/ERK signaling pathway participates in hyperalgesia central sensitization, thus implicating the MAPK/ERK signaling pathway in the occurrence and development of pain.[45–47] After components of this pathway is phosphorylated in the dorsal horn of the spinal cord, transcription factors are activated, gene transcription is regulated, and central sensitization and nerve injury pain are maintained, with phosphorylation of ERK and cAMP response element binding protein (CREB) reported to be involved in this process.[48–50] In this study, we show that GO analysis revealed enrichment of the MAPK signaling pathway in the BP category, and predicted the involvement of JNK and p38 by network pharmacology analysis. Analyses of the spinal cord tissues of formalin foot swelling model mice revealed that PC alcohol extract modulated the mRNA expressions and protein phosphorylation levels of p38, JNK, ERK, and CREB. These results indicate that PC exerts analgesic effects through the MAPK/ERK signaling pathway.

Conclusion

In this study, we identified the anti-inflammatory and analgesic effects of PC alcohol extracts in three different inflammatory pain models and demonstrated that their mechanism is related to the inhibition of the MAPK/ERK signaling pathway (Figure 7). However, although its application in the treatment of pain disorders is of potential interests, many questions

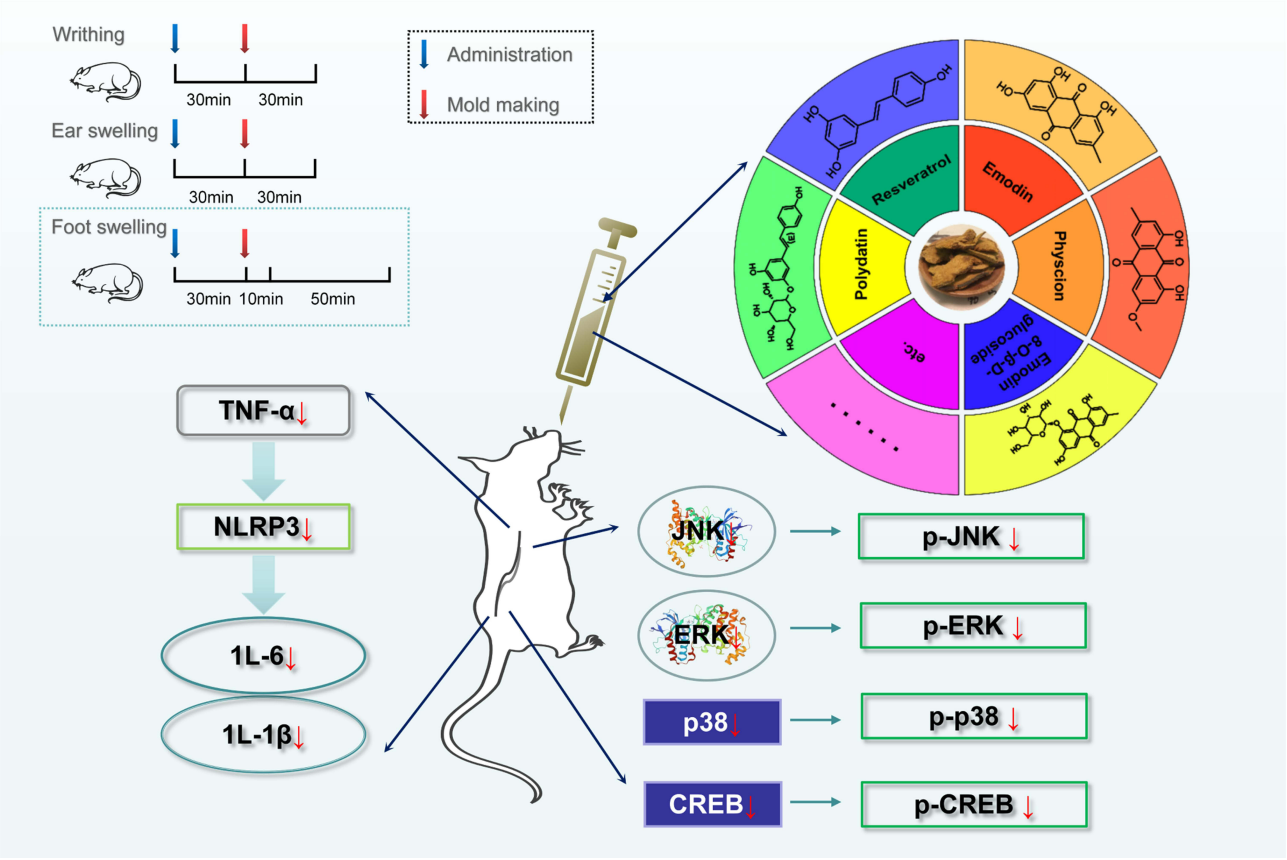

Figure 7 Mechanism by which PC alcohol extract exerts its analgesic effects through inflammation and via the MAPK/ERK signaling pathway.

need to be clarified, such as its possible effect on spinal synapses and neurons, as well as the underlying molecular mechanisms in addition to inhibition of MAPK pathways.

Data Sharing Statement

The datasets generated during and/or analyzed during the current study are available from the corresponding author on reasonable request.

Ethics Approval and Consent to Participate

All animal experiments were approved by the animal ethics committee of Hubei University of Chinese Medicine (license is No. SCXK 2019- 0002). Experiments were carried out according to the National Institutes of Health (United States) Guide for the Care and Use of Laboratory Animals.

Consent for Publication

All the listed authors have approved.

Author Contributions

All authors made substantial contributions to conception and design, acquisition of data, or analysis and interpretation of data; took part in drafting the article or revising it critically for important intellectual content; agreed to submit to the current journal; gave final approval of the version to be published; and agree to be accountable for all aspects of the work.

Funding

This work was supported by the Special Fund of Wu Jieping Medical Foundation for Clinical Scientific Research (320.6750.2021-10-106), Hubei Provincial Department of Education (Q20202006), Hubei Provincial Department of Science and Technology (2022CFD062), and Research Projects of Biomedical Center of Hubei Cancer Hospital.

Disclosure

The authors declare no competing of interest.

References

1. Guo YP, Zhi YR, Liu TT, et al. Global gene knockout of Kcnip3 enhances pain sensitivity and exacerbates negative emotions in rats. *Front Mol Neurosci*. 2019;12:5. doi:10.3389/fnmol.2019.00005
2. Adams JD. Pain and Inflammation. *Curr Med Chem*. 2020;27(9):1444–1445. doi:10.2174/0929867327092003270924 13
3. Qin F, Zhang H, Liu A, et al. Analgesic effect of Zanthoxylum *nitidum* extract in inflammatory pain models through targeting of ERK and NF-κB signaling. *Front Pharmacol*. 2019;10:359. doi:10.3389/fphar.2019.00359
4. Wang H, Xu C. A novel progress: glial cells and inflammatory pain. *ACS Chem Neurosci*. 2022;13(3):288–295. doi:10.1021/acschemneuro.1c00607
5. Quade BN, Parker MD, Occhipinti R. The therapeutic importance of acid-base balance. *Biochem Pharmacol*. 2021;183:114278.
6. Viswanath O, Urits I, Burns J, et al. Central neuropathic mechanisms in pain signaling pathways: current evidence and recommendations. *Adv Ther*. 2020;37(5):1946–1959.
7. De Feo M, Paladini A, Ferri C, et al. Anti-inflammatory and anti-nociceptive effects of cocoa: a review on future perspectives in treatment of pain. *Pain Ther*. 2020;9(1):231–240.
8. Tonkin RS, Bowles C, Perera CJ, et al. Attenuation of mechanical pain hypersensitivity by treatment with Peptide5, a connexin-43 mimetic peptide, involves inhibition of NLRP3 inflammasome in nerve-injured mice. *Exp Neurol*. 2018;300:1–12.
9. Cohen SP, Vase L, Hooten WM. Chronic pain: an update on burden, best practices, and new advances. *Lancet*. 2021;397(10289):2082–2097.
10. Kavaliers M, Ossenkopp KP, Tyson CD, et al. Social factors and the neurobiology of pathogen avoidance. *Biol Lett*. 2022;18(2):20210371.
11. Pan B, Shi X, Ding T, et al. Unraveling the action mechanism of Polygonum *cuspidatum* by a network pharmacology approach. *Am J Transl Res*. 2019;11(11):6790–6811.
12. Wu M, Li X, Wang S, et al. Polydatin for treating atherosclerotic diseases: a functional and mechanistic overview. *Biomed Pharmacother*. 2020;128:110308.
13. Xu HB, Yang YG, Xu HL, et al. Screening 5-lipoxygenase inhibitors from selected traditional Chinese medicines and isolation of the active compounds from Polygoni Cuspidati Rhizoma by an on-line bioactivity evaluation system. *Biomed Chromatogr*. 2022;36(9):e5426.
14. Zheng Y, Shi Y, Yang X, et al. Effects of resveratrol on lipid metabolism in liver of red tilapia Oreochromis niloticus. *Comp Biochem Physiol C Toxicol Pharmacol*. 2022;261:109408.
15. Zhao J, Li H, Shi C, et al. Electroacupuncture inhibits the activity of astrocytes in spinal cord in rats with visceral hypersensitivity by inhibiting P2Y(1) receptor-mediated MAPK/ERK signaling pathway. *Evid Based Complement Alternat Med*. 2020;2020:4956179.

16. He JR, Yu SG, Tang Y, et al. Purinergic signaling as a basis of acupuncture-induced analgesia. *Purinergic Signal*. 2020;16(3):297–304.
17. GonçalvesDos Santos G, Delay L, Yaksh TL, et al. Neuraxial cytokines in pain states. *Front Immunol*. 2019;10:3061.
18. Juncheng L, Deyong Z. Experimental study on the treatment of acute gouty arthritis with hongteng and Polygonum *cuspidatum* compound free decoction. *Yunnan J Tradit Chin Med Materia Med*. 2018;39(09):75–76.
19. Juanjuan T. Analgesic effect of Polygonum *cuspidatum* extract in rat model of neuropathic pain. *Chin J Mod Drug Appl*. 2014;8(07):1–3.
20. Dexuan K, Yunzhong C, Yingrui Z, et al. Study on relationship between HPLC fingerprint of Polygonum cuspidatum and active spectrum of anti gouty arthritis. *Chin Tradit Herb Drugs*. 2022;53(02):569–574.
21. Yingrui Z, Dexuan K, Weiran Z, et al. Optimization of drying process of Polygonum cuspidatum by multi-index evaluation method and correlation analysis between its extract and color difference. *Lishizhen Med Mat Med Res*. 2020;31(11):2626–2629.
22. Bokhovchuk F, Mesrouze Y, Izaac A, et al. Molecular and structural characterization of a TEAD mutation at the origin of Sveinsson's chorioretinal atrophy. *Febs j*. 2019;286(12):2381–2398.
23. Yuri K, Erich H, Cassidy KC, et al. Webina: an open-source library and web app that runs autodock vina entirely in the web browser. *Bioinformatics*. 2020;36(16):4513–4515.
24. Hu N, Wang C, Wang B, et al. Qianghuo Shengshi decoction exerts anti-inflammatory and analgesic via MAPKs/CREB signaling pathway. *J Ethnopharmacol*. 2022;284:114776.
25. Chen Y, Xu E, Sang M, et al. Makatoxin-3, a thermostable Nav1.7 agonist from Buthus martensii Karsch (BmK) scorpion elicits non-narcotic analgesia in inflammatory pain models. *J Ethnopharmacol*. 2022;288:114998.
26. Xu J, Zhou L, Sun L, et al. 3α-Angeloyloxy-ent-kaur-16-en-19-oic acid isolated from wedelia trilobata L. Alleviates xylene-induced mouse ear edema and inhibits NF-κB and MAPK Pathway in LPS-stimulated macrophages. *J Nat Prod*. 2020;83(12):3726–3735.
27. Chun-Xiao L, Shan-Shan W, Shu-Jing C, et al. Research development on chemical composition and pharmacology of polygoni cuspidati rhizoma et radix. *Chin Tradit Herb Drugs*. 2022;53(04):1264–1276.
28. Chen C, Lin Z, Liu W, et al. Emodin accelerates diabetic wound healing by promoting anti-inflammatory macrophage polarization. *Eur J Pharmacol*. 2022;936:175329.
29. Dong X, Wang L, Song G, et al. Physcion protects rats against cerebral ischemia-reperfusion injury via inhibition of TLR4/NF-kB signaling pathway. *Drug Des Devel Ther*. 2021;15:277–287.
30. Liu W, Chen P, Deng J, et al. Resveratrol and polydatin as modulators of Ca(2+) mobilization in the cardiovascular system. *Ann N Y Acad Sci*. 2017;1403(1):82–91.
31. Wang P, He Q, Zhu J. Emodin-8-O-glucuronic acid, from the traditional Chinese medicine qinghuobaiduyin, affects the secretion of inflammatory cytokines in LPS-stimulated raw 264.7 cells via HSP70. *Mol Med Rep*. 2016;14(3):2368–2372.
32. Fu J, Wu S, Wang M, et al. Intestinal metabolism of Polygonum cuspidatum in vitro and in vivo. *Biomed Chromatogr*. 2018;32(6):e4190.
33. Xu H, Li J, Song S, et al. Effective inhibition of coronavirus replication by Polygonum cuspidatum. *Front Biosci*. 2021;26(10):789–798.
34. Fan W, Chen S, Wu X, et al. Resveratrol relieves gouty arthritis by promoting mitophagy to inhibit activation of NLRP3 inflammasomes. *J Inflamm Res*. 2021;14:3523–3536.
35. Chang WC, Chu MT, Hsu CY, et al. Rhein, an anthraquinone drug, suppresses the NLRP3 Inflammasome and macrophage activation in urate crystal-induced gouty inflammation. *Am J Chin Med*. 2019;47(1):135–151.
36. Fan H, Wu Z, Zhu D, et al. Proanthocyanidins Inhibit the transmission of spinal pain information through a presynaptic mechanism in a mouse inflammatory pain model. *Front Neurosci*. 2021;15:804722.
37. Fu WJ, Tang JJ, Wang H, et al. In vivo and in vitro anti-sepsis effects of physcion 8-O-β-glucopyranoside extracted from Rumex japonicus. *Chin J Nat Med*. 2017;15(7):534–539.
38. Sharifi-Rad J, Herrera-Bravo J, Kamiloglu S, et al. Recent advances in the therapeutic potential of emodin for human health. *Biomed Pharmacother*. 2022;154:113555.
39. Szkudelska K, Szkudelski T. Resveratrol, obesity and diabetes. *Eur J Pharmacol*. 2010;635(1–3):1–8.
40. Di Benedetto A, Posa F, De Maria S, et al. Polydatin, natural precursor of resveratrol, promotes osteogenic differentiation of mesenchymal stem cells. *Int J Med Sci*. 2018;15(9):944–952.
41. Farrell SF, De Zoete RMJ, Cabot PJ, et al. Systemic inflammatory markers in neck pain: a systematic review with meta-analysis. *Eur J Pain*. 2020;24(9):1666–1686.
42. Ding W, You Z, Chen Q, et al. Gut microbiota influences neuropathic pain through modulating proinflammatory and anti-inflammatory T cells. *Anesth Analg*. 2021;132(4):1146–1155.
43. Ronchetti S, Migliorati G, Delfino DV. Association of inflammatory mediators with pain perception. *Biomed Pharmacother*. 2017;96:1445–1452.
44. Wang R, Tao L, Lu Q, et al. The analgesic activities of total alkaloids of the ethnic medicine Cynanchum komarovii Al. Iljinski. *J Ethnopharmacol*. 2022;285:114861.
45. Nishino T, Tamada K, Maeda A, et al. Behavioral analysis in mice deficient for GAREM2 (Grb2-associated regulator of Erk/MAPK subtype2) that is a subtype of highly expressing in the brain. *Mol Brain*. 2019;12(1):94.
46. Sun Y, Zhang L, Zhang M, et al. Characterization of three mitogen-activated protein kinases (MAPK) genes reveals involvement of ERK and JNK, not p38 in defense against bacterial infection in Yesso scallop Patinopecten yessoensis. *Fish Shellfish Immunol*. 2016;54:507–515.
47. Wang Y, Wang X, Qi R, et al. Interleukin 33-mediated inhibition of A-type K(+) channels induces sensory neuronal hyperexcitability and nociceptive behaviors in mice. *Theranostics*. 2022;12(5):2232–2247.
48. Ma Y, Zhang X, Li C, et al. Spinal N-Cadherin/CREB signaling contributes to chronic alcohol consumption-enhanced postsurgical pain. *J Pain Res*. 2020;13:2065–2072.
49. Wang B, Liu S, Fan B, et al. PKM2 is involved in neuropathic pain by regulating ERK and STAT3 activation in rat spinal cord. *J Headache Pain*. 2018;19(1):7.
50. Zhang J, Li Z, Chen F, et al. TGF-β1 suppresses CCL3/4 expression through the ERK signaling pathway and inhibits intervertebral disc degeneration and inflammation-related pain in a rat model. *Exp Mol Med*. 2017;49(9):e379.